

# Radiative transfer and multiple scattering of diffuse ultrasound in polycrystalline media

**Joseph A. Turner and Richard L. Weaver**  
*Department of Theoretical and Applied Mechanics*  
*University of Illinois at Urbana-Champaign*  
*Urbana, IL 61801*

## Abstract

*A model is presented for the multiply scattered incoherent field in a continuous polycrystalline elastic medium. Unlike a previous development based upon energy conservation considerations [J.A. Turner and R.L. Weaver, J. Acoust. Soc. Am., 93, 2312 (A) 1993] for a medium containing discrete random scatterers, the present model has been developed from the wave equation and first principles. Appropriate ensemble averaging of the wave equation leads to Dyson and Bethe-Salpeter equations which govern the mean Green's function and the covariance of the Green's function, respectively. These equations are expanded for weak heterogeneity and equations of radiative transfer are obtained. The result is valid for attenuations that are small compared to a wave number:  $\alpha/k \ll 1$ . Polarization effects are included, as before, through five elastodynamic Stokes parameters, one longitudinal and four shear. The theory is applied to a statistically homogeneous and statistically isotropic half-space composed of cubic crystallites illuminated by a plane wave. Results for the angular dependence of backscattered intensity are presented. It is anticipated that this approach may be applicable to microstructural characterization through the study of the time, space, ultrasonic frequency, and angular dependence of multiply scattered ultrasound in elastic media.*

Submitted for publication to the *Journal of the Acoustical Society of America*



## INTRODUCTION

The use of ultrasound for microstructural characterization of polycrystalline materials can be traced to the late 1940's and the work of Mason and McSkimm.<sup>1</sup> Their work and much of the work which followed<sup>2,3,4,5</sup> relied on the use of coherent fields for inferring microstructural information from measured attenuations and wave speeds. Current research efforts have also involved the use of diffuse or incoherent speckle fields.<sup>6,7,8,9,10,11</sup> Diffuse field experiments have less stringent geometric requirements (e.g. parallel surfaces) than coherent field experiments. It is thus thought that the use of diffuse fields may be a more effective microstructural characterization tool for field measurements.

Much of the theory used to describe the scattering of these diffuse fields has been limited to weakly scattering materials so that single scattering theories suffice<sup>9,10,11</sup> or to diffusive limits.<sup>12,13</sup> The multiply scattered fields between these two limits, however, contain a wealth of information about the scattering medium such as absorption information which is unavailable in the singly scattered fields. These fields thus provide a more complete description of the scattering medium and may provide a more powerful microstructural characterization tool. The task at hand, then, is to develop an accurate model for the multiply scattered diffuse intensity.

Recently, a method was proposed to model ultrasonic multiple scattering effects in a medium containing randomly located discrete scatterers using radiative transfer theory.<sup>14</sup> An ultrasonic radiative transfer equation (URTE) was derived using energy balance considerations similar to those used in electromagnetic radiative transfer theory.<sup>15,16,17</sup> This equation governs the propagation and scattering of the five elastic Stokes parameters, one longitudinal and four shear, that are needed to describe the diffuse intensities completely. The URTE has as a parameter a Mueller matrix which defines the scatterings between the different Stokes parameters. For discrete scatterers this matrix is derived from an examination of the scattering from a single

scatterer. For a continuous medium, however, the choice of a representative scatterer is not apparent. Therefore, a more fundamental examination of ensemble average responses is required to obtain the governing URTE. This was done by Weaver<sup>13</sup> in his derivation of an expression for the properties of the diffusion limit.

In the next section the ultrasonic radiative transfer equation is discussed as given by Weaver.<sup>13</sup> In section II, this equation is put into a form identical to the URTE derived for the case of randomly located discrete scatterers.<sup>14</sup> Finally, in section III, solution techniques derived for the discrete scatterer case are used to solve the polycrystalline URTE and results presented.

## I. RADIATIVE TRANSFER THEORY

An examination of stochastic operator theory as given by Karal and Keller,<sup>18</sup> Frisch,<sup>19</sup> McCoy,<sup>20</sup> and others was the starting point for the derivation of the polycrystalline ultrasonic radiative transfer equation (URTE) given by Weaver.<sup>13</sup> His development is summarized here for completeness and clarity.

The elastodynamic wave equation was considered with moduli that are random in space and given by

$$C_{ijkl}(\mathbf{x}) = C_{ijkl}^0 + \gamma_{ijkl}(\mathbf{x}) \quad (1)$$

where the brackets  $\langle \rangle$  denote an ensemble average,  $C_{ijkl}^0$  are the Voigt-average moduli, and  $\gamma_{ijkl}$  is the randomly fluctuating part of the moduli which has an ensemble average of zero. The covariance of the moduli fluctuations is given by

$$\langle \gamma_{\alpha\beta\gamma\delta}(\mathbf{x}) \gamma_{ijkl}(\mathbf{x}') \rangle = \Xi_{ijkl}^{\alpha\beta\gamma\delta} \eta(|\mathbf{x} - \mathbf{x}'|), \quad (2)$$

where  $\Xi$  is the tensorial part of the covariance and  $\eta$  is the dimensional two-point correlation function defined as  $v^2$  times the probability that two points in the medium separated by a distance



$r = |\mathbf{x} - \mathbf{x}'|$  lie within the same crystallite. For a crystallite with cubic symmetry,  $\nu = C_{11} - C_{12} - 2C_{44}$ , where the  $C$ 's are the elastic constants. The implicit assumptions included in Eq. (2) are statistical homogeneity, statistical isotropy, and that orientations between different crystallites are uncorrelated.<sup>13</sup> No further assumptions about the two-point correlation function are made at this time but an exponential form is used for the numerical results presented in section III. Higher order statistical information about the medium is assumed negligible compared to the covariance.<sup>13</sup>

When one considers the ensemble average responses of the temporally Fourier transformed wave equation, with transform variable  $\omega$ , one arrives at two integral equations that govern the lowest order statistics of the Green's dyadic.<sup>13</sup> The Dyson equation

$$\langle G_{i\alpha}(\mathbf{x}, \mathbf{x}') \rangle = G_{i\alpha}^0(\mathbf{x}, \mathbf{x}') + \int \int G_{i\beta}^0(\mathbf{x}, \mathbf{y}) m_{\beta j}(\mathbf{y}, \mathbf{z}) \langle G_{j\alpha}(\mathbf{z}, \mathbf{x}') \rangle d^3 y d^3 z, \quad (3)$$

governs the mean Green's dyadic,  $\langle \mathbf{G} \rangle$ , where  $\mathbf{G}^0$  is the Voigt-average Green's dyadic and  $\mathbf{m}$  is the mass operator. The Bethe-Salpeter equation

$$\langle G_{\alpha\beta}(\mathbf{x}, \mathbf{x}') G_{ij}^*(\mathbf{y}, \mathbf{y}') \rangle = \langle G_{\alpha\beta}(\mathbf{x}, \mathbf{x}') \rangle \langle G_{ij}(\mathbf{y}, \mathbf{y}') \rangle + \int \int \int \langle G_{\alpha\gamma}(\mathbf{x}, \mathbf{z}) \rangle \langle G_{ik}^*(\mathbf{x}', \mathbf{z}') \rangle {}_k K_l^\delta(\mathbf{z}, \mathbf{z}', \mathbf{w}, \mathbf{w}') \langle G_{\delta\beta}(\mathbf{w}, \mathbf{y}) G_{lj}^*(\mathbf{w}', \mathbf{y}') \rangle d^3 \mathbf{z} d^3 \mathbf{z}' d^3 \mathbf{w} d^3 \mathbf{w}', \quad (4)$$

governs the covariance of the Green's dyadic,  $\langle \mathbf{G} \mathbf{G}^* \rangle$ , where  $\mathbf{K}$  is the intensity operator and the asterisk denotes a complex conjugate.

It should be noted that there are two time scales involved in these equations and thus two temporal transform variables are needed. The inner frequency,  $\omega$ , is the ultrasonic excitation frequency which appears in the transformed wave equation and is implicit in the Green's dyadics given in Eqs. (3) and (4). The diffuse intensity, which is proportional to the covariance, evolves with respect to a slower time scale. It transforms to the outer frequency,  $\Omega$ , implicit in the

complex conjugate of the Green's dyadic,  $\mathbf{G}^*$ , evaluated at  $\omega + \Omega$ . A similar distinction may be drawn between inner wave number (here designated by the symbols  $\mathbf{s}$  and  $\mathbf{p}$ ) characteristic of the waves, and outer wave numbers,  $\Delta$ , characteristic of the spatial variation of the diffuse intensity.

The Dyson and Bethe-Salpeter equations are Fourier transformed in space to simplify further analysis. The operators,  $\mathbf{m}$  and  $\mathbf{K}$ , are then simplified by means of the First-Order Smoothing Approximation (FOSA) and found to be proportional to  $\Xi\eta$ . As outlined by Frisch and extended to the dyadic case by Weaver, the FOSA allows approximation of  $\mathbf{m}$  and  $\mathbf{K}$  to lowest order in fluctuating moduli,  $\gamma$ . Finally, an approximation is used which limits the validity of the results to frequencies below the geometrical optics limit. Within the context of these assumptions, the Dyson equation is solved exactly for the mean Green's dyadic. The Bethe-Salpeter equation, in the radiative transfer limit in which attenuations are much smaller than an inner wave number, reduces to a radiative transfer equation for the source function,  $\mathbf{S}$ ,

$$\mathbf{S}(\mathbf{p}) = \mathbf{I} + \int d^2\hat{s} \hat{s}^{\mathbf{p}} \mathbf{K}_{\hat{s}\omega/c_L}^{\hat{s}\omega/c_L \cdot \hat{s}\hat{s}} \cdot \mathbf{S}(\hat{s}\omega/c_L) R^L(\hat{s}) + \hat{s}^{\mathbf{p}} \mathbf{K}_{\hat{s}\omega/c_T}^{\hat{s}\omega/c_T \cdot \mathbf{I} - \hat{s}\hat{s}} \cdot \mathbf{S}(\hat{s}\omega/c_T) R^T(\hat{s}). \quad (5)$$

The second rank tensor,  $\mathbf{S}$ , represents sources of radiant intensity and is a function of the direction of propagation,  $\hat{\mathbf{p}}$ , the spatial Fourier transform variable,  $\Delta$ , and both inner and outer frequencies,  $\omega$  and  $\Omega$ . The energy propagators,  $R^L$  and  $R^T$ , for the longitudinal and transverse modes, respectively, are functions of  $\hat{\mathbf{p}}$ ,  $\Delta$ , and  $\Omega$ . The approximated spatially transformed intensity operator,  $\mathbf{K}$ , is given by

$$\hat{s}^{\mathbf{p}} \gamma \mathbf{K}_{ls}^{\delta s} = \tilde{\eta}(\mathbf{p} - \mathbf{s}) p_{\mathbf{p}} s_{\alpha} p_i s_j \Xi_{ijkl}^{\alpha\beta\gamma\delta}, \quad (6)$$

where  $\mathbf{p}$  and  $\mathbf{s}$  are spatial Fourier transform wave vectors,  $\Xi$  is defined in Eq. (2), and  $\tilde{\eta}$  is the spatial transform of the dimensional two-point correlation function defined by

$$\tilde{\eta}(\mathbf{q}) = \frac{1}{(2\pi)^3} \int \eta(\mathbf{r}) e^{-i\mathbf{q} \cdot \mathbf{r}} d^3r. \quad (7)$$

From Eq. (5) it can be seen that sources of radiant intensity are equal to a primary contribution,  $\mathbf{I}$ , and secondary contributions from scatterings of the sources from the  $\hat{\mathbf{s}}$  direction into the  $\hat{\mathbf{p}}$  direction. The primary source,  $\mathbf{I}$ , is neglected here. Weaver further approximated the source function in order to simplify Eq. (5) in conjunction with a diffusive limit to derive the diffusivity for polycrystalline media.

The assumptions used in the derivation of Eq. (5) are by no means prohibitive for most materials of interest. The assumptions used for the definition of the covariance of the moduli fluctuation given in Eq. (2) are easily satisfied for a large class of commonly used materials as is the requirement of weak material heterogeneity. The radiative transfer limit in which it was assumed that attenuation is weak over distances of the order of a wavelength over  $2\pi$  is equivalent to the assumption of weak material heterogeneity. Thus, Eq. (5) should represent reasonably well the multiple scattering effects of diffuse intensities within polycrystalline materials.

Eq. (5) is the starting point for the present communication. It is now put into a form identical to the ultrasonic radiative transfer equation derived previously for a medium containing discrete scatterers.<sup>14</sup>

## II. ULTRASONIC RADIATIVE TRANSFER EQUATION

From the derivation of the URTE for the discrete scatterer case,<sup>14</sup> we know that five Stokes parameters, one longitudinal and four shear, are needed to characterize the diffuse intensity completely. Thus, we begin by expanding  $\mathbf{S}$  in terms of five independent dyadics as

$$\mathbf{S}(\mathbf{p}) = S_L(\hat{\mathbf{p}})\hat{\mathbf{p}}\hat{\mathbf{p}} + S_{SV}(\hat{\mathbf{p}})\hat{\mathbf{p}}_2\hat{\mathbf{p}}_2 + S_{SH}(\hat{\mathbf{p}})\hat{\mathbf{p}}_3\hat{\mathbf{p}}_3 + P(\hat{\mathbf{p}})\hat{\mathbf{p}}_2\hat{\mathbf{p}}_3 + Q(\hat{\mathbf{p}})\hat{\mathbf{p}}_3\hat{\mathbf{p}}_2, \quad (8)$$

where  $\hat{\mathbf{p}}$  is the direction of propagation and  $(\hat{\mathbf{p}}, \hat{\mathbf{p}}_2, \hat{\mathbf{p}}_3)$  is an orthonormal triad used to resolve the five distinct elements of  $\mathbf{S}$ . The five elements of  $\mathbf{S}$ ,  $S_L$ ,  $S_{SV}$ ,  $S_{SH}$ ,  $P$ , and  $Q$  are a kind of source-like

Stokes parameters. The four remaining elements of the tensor  $\mathbf{S}$ , which are neglected here, represent the coherent interference between longitudinal and transverse modes which is destroyed after short distances of propagation due to the difference in wave speeds.<sup>13,14</sup>

Substituting this form of  $\mathbf{S}$  into Eq. (5) gives

$$S_L \hat{\mathbf{p}}\hat{\mathbf{p}} + S_{SV} \hat{\mathbf{p}}_2\hat{\mathbf{p}}_2 + S_{SH} \hat{\mathbf{p}}_3\hat{\mathbf{p}}_3 + P \hat{\mathbf{p}}_2\hat{\mathbf{p}}_3 + Q \hat{\mathbf{p}}_3\hat{\mathbf{p}}_2 = \int d^2\hat{s} \left\{ \mathbf{K}_{\hat{\mathbf{p}}\hat{\mathbf{p}}/c_L}^{\hat{\mathbf{p}}\hat{\mathbf{p}}/c_L} S_L R^L(\hat{\mathbf{s}}) + \mathbf{K}_{\hat{\mathbf{p}}\hat{\mathbf{p}}/c_T}^{\hat{\mathbf{p}}\hat{\mathbf{p}}/c_T} \left[ \hat{s}_2 S_{SV} + \hat{s}_3 S_{SH} + \hat{s}_2 P + \hat{s}_3 Q \right] R^T(\hat{\mathbf{s}}) \right\}. \quad (9)$$

Eq. (9) may be contracted onto each of the dyadics  $\hat{\mathbf{p}}\hat{\mathbf{p}}$ ,  $\hat{\mathbf{p}}_2\hat{\mathbf{p}}_2$ ,  $\hat{\mathbf{p}}_3\hat{\mathbf{p}}_3$ ,  $\hat{\mathbf{p}}_2\hat{\mathbf{p}}_3$ , and  $\hat{\mathbf{p}}_3\hat{\mathbf{p}}_2$ . This results in five scalar equations. Each contraction reduces the left-hand side to a single parameter and the right-hand side to a sum of the five Stokes-source parameters multiplied by an appropriate inner product on the intensity operator,  $\mathbf{K}$ , and an appropriate energy propagator. These five equations are

$$\frac{I_L}{R^L c_L} = \int d^2\hat{s} \left[ \frac{\omega^4}{c_L^5} \eta^{LL}(\Theta)_{\hat{\mathbf{p}}\hat{\mathbf{p}}\hat{\mathbf{s}}\hat{\mathbf{s}}} \Xi I_L + \frac{\omega^4}{c_L^2 c_T^3} \eta^{LT}(\Theta)_{\hat{\mathbf{p}}\hat{\mathbf{p}}\hat{\mathbf{s}}_2\hat{\mathbf{s}}_3} \Xi I_{SV} + \frac{\omega^4}{c_L^2 c_T^3} \eta^{LT}(\Theta)_{\hat{\mathbf{p}}\hat{\mathbf{p}}\hat{\mathbf{s}}_3\hat{\mathbf{s}}_2} \Xi I_{SH} + \frac{\omega^4}{c_L^2 c_T^3} \eta^{LT}(\Theta)_{\hat{\mathbf{p}}\hat{\mathbf{p}}\hat{\mathbf{s}}_2\hat{\mathbf{s}}_3} \Xi I_P + \frac{\omega^4}{c_L^2 c_T^3} \eta^{LT}(\Theta)_{\hat{\mathbf{p}}\hat{\mathbf{p}}\hat{\mathbf{s}}_3\hat{\mathbf{s}}_2} \Xi I_Q \right], \quad (10)$$

$$\frac{I_{SV}}{R^T c_T} = \int d^2\hat{s} \left[ \frac{\omega^4}{c_L^3 c_T^2} \eta^{TL}(\Theta)_{\hat{\mathbf{p}}_2\hat{\mathbf{p}}_2\hat{\mathbf{s}}\hat{\mathbf{s}}} \Xi I_L + \frac{\omega^4}{c_T^5} \eta^{TT}(\Theta)_{\hat{\mathbf{p}}_2\hat{\mathbf{p}}_2\hat{\mathbf{s}}_2\hat{\mathbf{s}}_2} \Xi I_{SV} + \frac{\omega^4}{c_T^5} \eta^{TT}(\Theta)_{\hat{\mathbf{p}}_2\hat{\mathbf{p}}_2\hat{\mathbf{s}}_3\hat{\mathbf{s}}_3} \Xi I_{SH} + \frac{\omega^4}{c_T^5} \eta^{TT}(\Theta)_{\hat{\mathbf{p}}_2\hat{\mathbf{p}}_2\hat{\mathbf{s}}_2\hat{\mathbf{s}}_3} \Xi I_P + \frac{\omega^4}{c_T^5} \eta^{TT}(\Theta)_{\hat{\mathbf{p}}_2\hat{\mathbf{p}}_2\hat{\mathbf{s}}_3\hat{\mathbf{s}}_2} \Xi I_Q \right], \quad (11)$$

$$\frac{I_{SH}}{R^T c_T} = \int d^2\hat{s} \left[ \frac{\omega^4}{c_L^3 c_T^2} \eta^{TL}(\Theta)_{\hat{\mathbf{p}}_3\hat{\mathbf{p}}_3\hat{\mathbf{s}}\hat{\mathbf{s}}} \Xi I_L + \frac{\omega^4}{c_T^5} \eta^{TT}(\Theta)_{\hat{\mathbf{p}}_3\hat{\mathbf{p}}_3\hat{\mathbf{s}}_2\hat{\mathbf{s}}_2} \Xi I_{SV} + \frac{\omega^4}{c_T^5} \eta^{TT}(\Theta)_{\hat{\mathbf{p}}_3\hat{\mathbf{p}}_3\hat{\mathbf{s}}_3\hat{\mathbf{s}}_3} \Xi I_{SH} + \frac{\omega^4}{c_T^5} \eta^{TT}(\Theta)_{\hat{\mathbf{p}}_3\hat{\mathbf{p}}_3\hat{\mathbf{s}}_2\hat{\mathbf{s}}_3} \Xi I_P + \frac{\omega^4}{c_T^5} \eta^{TT}(\Theta)_{\hat{\mathbf{p}}_3\hat{\mathbf{p}}_3\hat{\mathbf{s}}_3\hat{\mathbf{s}}_2} \Xi I_Q \right], \quad (12)$$



$$\frac{I_P}{R^T c_T} = \int d^2 \hat{s} \left[ \frac{\omega^4}{c_L^3 c_T^2} \eta^{TL}(\Theta)_{\hat{p}_3 \hat{p}_{ss} \dots} \Xi I_L + \frac{\omega^4}{c_T^5} \eta^{TT}(\Theta)_{\hat{p}_3 \hat{p}_{ss_2} \dots} \Xi I_{SV} + \right. \\ \left. \frac{\omega^4}{c_T^5} \eta^{TT}(\Theta)_{\hat{p}_3 \hat{p}_{ss_3} \dots} \Xi I_{SH} + \frac{\omega^4}{c_T^5} \eta^{TT}(\Theta)_{\hat{p}_3 \hat{p}_{ss_2} \dots} \Xi I_P + \frac{\omega^4}{c_T^5} \eta^{TT}(\Theta)_{\hat{p}_3 \hat{p}_{ss_2} \dots} \Xi I_Q \right], \quad (13)$$

$$\frac{I_Q}{R^T c_T} = \int d^2 \hat{s} \left[ \frac{\omega^4}{c_L^3 c_T^2} \eta^{TL}(\Theta)_{\hat{p}_2 \hat{p}_{ss} \dots} \Xi I_L + \frac{\omega^4}{c_T^5} \eta^{TT}(\Theta)_{\hat{p}_2 \hat{p}_{ss_2} \dots} \Xi I_{SV} + \right. \\ \left. \frac{\omega^4}{c_T^5} \eta^{TT}(\Theta)_{\hat{p}_2 \hat{p}_{ss_3} \dots} \Xi I_{SH} + \frac{\omega^4}{c_T^5} \eta^{TT}(\Theta)_{\hat{p}_2 \hat{p}_{ss_2} \dots} \Xi I_P + \frac{\omega^4}{c_T^5} \eta^{TT}(\Theta)_{\hat{p}_2 \hat{p}_{ss_2} \dots} \Xi I_Q \right], \quad (14)$$

where

$$I_L = S_L c_L R^L, \quad I_{SV} = S_{SV} c_T R^T, \quad I_{SH} = S_{SH} c_T R^T, \\ I_P = S_P c_T R^T, \quad I_Q = S_Q c_T R^T, \quad (15)$$

define the specific intensities. The  $\eta$  factors given in Eqs. (10)-(14) are the spatially Fourier transformed dimensional two-point correlation functions defined as

$$\eta^{LL}(\Theta) = \tilde{\eta}(\hat{p}\omega/c_L - \hat{s}\omega/c_L), \quad \eta^{TT}(\Theta) = \tilde{\eta}(\hat{p}\omega/c_T - \hat{s}\omega/c_T), \\ \eta^{LT}(\Theta) = \eta^{TL}(\Theta) = \tilde{\eta}(\hat{p}\omega/c_L - \hat{s}\omega/c_T), \quad (16)$$

where  $\Theta$  is the angle separating the incident and scattered directions,  $\hat{s}$  and  $\hat{p}$ , respectively and  $\tilde{\eta}$  is defined in Eq. (7).

With the definitions of the specific intensities given in Eq. (15), the energy density given in Eq. (6.4) of Weaver and the flux given in his Eq. (6.5) agree with the energy density and flux found using the Stokes parameters defined for discrete scatterers.<sup>14</sup>

The energy propagators,  $R^L$  and  $R^T$ , are given by

$$\frac{1}{R^L c_L} = \frac{2c_L^3}{\pi} \left[ \kappa_L + \frac{i\Omega}{c_L} - i\hat{\mathbf{p}} \cdot \Delta \right], \quad \frac{1}{R^T c_T} = \frac{2c_T^3}{\pi} \left[ \kappa_T + \frac{i\Omega}{c_T} - i\hat{\mathbf{p}} \cdot \Delta \right], \quad (17)$$

where  $\kappa_L$  and  $\kappa_T$  are the longitudinal and transverse coherent intensity attenuations, respectively,  $\Omega$  the outer frequency, and  $\Delta$  the spatial Fourier transform vector. Eqs. (17) reduce to those given by Weaver in the diffusion limit,  $\Delta \ll \kappa$  and  $\Omega \ll \kappa c$ . In the inverse transform domain both  $R^L$  and  $R^T$  are then

$$\frac{1}{R^L c_L} = \frac{2c_L^3}{\pi} \left[ \kappa_L + \frac{1}{c_L} \frac{\partial}{\partial t} + \hat{\mathbf{p}} \cdot \nabla \right], \quad \frac{1}{R^T c_T} = \frac{2c_T^3}{\pi} \left[ \kappa_T + \frac{1}{c_T} \frac{\partial}{\partial t} + \hat{\mathbf{p}} \cdot \nabla \right]. \quad (18)$$

These expressions for the energy propagators allow Eqs. (10)-(14) to be written in a form similar to that for discrete scatterers<sup>14</sup>

$$\nabla \cdot \hat{\mathbf{p}} \underline{I}(\mathbf{r}, t, \hat{\mathbf{p}}) + \underline{c}^{-1} \frac{\partial \underline{I}(\mathbf{r}, t, \hat{\mathbf{p}})}{\partial t} + (\underline{\kappa} + \underline{\nu}) \underline{I}(\mathbf{r}, t, \hat{\mathbf{p}}) = \frac{1}{4\pi} \int \underline{P}(\hat{\mathbf{p}}, \hat{\mathbf{p}}') \underline{I}(\mathbf{r}, t, \hat{\mathbf{p}}') d^2 \hat{\mathbf{p}}', \quad (19)$$

where  $\underline{I}$  is the Stokes vector containing the five Stokes parameters defined in Eq. (15), and  $\underline{c}$ ,  $\underline{\kappa}$ , and  $\underline{\nu}$  define the wave speed, attenuation, and absorption matrices, respectively, given by

$$\underline{c} = \begin{bmatrix} c_L & 0 & 0 & 0 & 0 \\ 0 & c_T & 0 & 0 & 0 \\ 0 & 0 & c_T & 0 & 0 \\ 0 & 0 & 0 & c_T & 0 \\ 0 & 0 & 0 & 0 & c_T \end{bmatrix}, \quad \underline{\kappa} = \begin{bmatrix} \kappa_L & 0 & 0 & 0 & 0 \\ 0 & \kappa_T & 0 & 0 & 0 \\ 0 & 0 & \kappa_T & 0 & 0 \\ 0 & 0 & 0 & \kappa_T & 0 \\ 0 & 0 & 0 & 0 & \kappa_T \end{bmatrix}, \quad \underline{\nu} = \begin{bmatrix} \nu_L & 0 & 0 & 0 & 0 \\ 0 & \nu_T & 0 & 0 & 0 \\ 0 & 0 & \nu_T & 0 & 0 \\ 0 & 0 & 0 & \nu_T & 0 \\ 0 & 0 & 0 & 0 & \nu_T \end{bmatrix}. \quad (20)$$

We have included an absorption matrix,  $\underline{\nu}$ , phenomenologically, while the  $1/4\pi$  in the definition of  $\underline{P}$  is included for consistency with the URTE derived for discrete scatterers. The elements of  $\underline{P}/4\pi$  are implicitly defined in Eqs. (10)-(14).

One particular medium for which the URTE will be solved is that of a plane-parallel medium shown in Figure 1. The scattering medium extends infinitely in the  $+z$  direction and in the  $\pm x$  and  $\pm y$  directions. Two angular variables,  $\phi$  and  $\mu$ , are needed to define the directional dependence of the intensities. The angle  $\phi$  is measured within the  $x$ - $y$  plane from the  $x$  axis in a right-hand sense while  $\mu = \cos \theta$ .

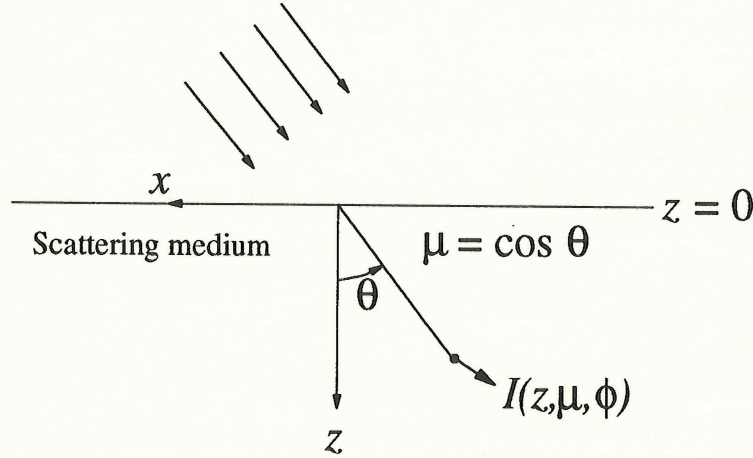


Figure 1. Geometry of a plane-parallel medium.

In the steady-state case, the Stokes vector is thus dependent upon  $z$ ,  $\mu$ , and  $\phi$  and Eq. (19) reduces to

$$\mu \frac{\partial \underline{I}(z, \mu, \phi)}{\partial z} + (\underline{\kappa} + \underline{\nu}) \underline{I}(z, \mu, \phi) = \frac{1}{4\pi} \int_{-1}^{+1} \int_0^{2\pi} \underline{P}(\mu, \phi; \mu', \phi') \underline{I}(z, \mu', \phi') d\mu' d\phi'. \quad (21)$$

The elements of the  $5 \times 5$  Mueller matrix,  $\underline{P}$ , depend on the  $\eta$  functions given in Eq. (16) and certain inner products between  $\Xi$  and the basis vectors of the orthonormal triad. As outlined previously,<sup>14,17</sup> the Mueller matrix can be constructed by first examining the scattering in a

locally defined coordinate system giving the scattering matrix  $\underline{\underline{F}}$ . Certain rotations on this local scattering matrix are used to create the Mueller matrix defined in the global coordinate system.

The Mueller matrix is thus given by<sup>14</sup>

$$\underline{\underline{P}}(\mu, \phi; \mu', \phi') = \underline{\underline{L}}(\gamma - 3\pi/2) \underline{\underline{F}}(\chi) \underline{\underline{L}}(\beta + \pi/2), \quad (22)$$

where the rotation matrices,  $\underline{\underline{L}}$ , are discussed elsewhere<sup>14</sup> and  $\chi$ ,  $\gamma$ , and  $\beta$  are functions of  $\mu$ ,  $\phi$ ,  $\mu'$ , and  $\phi'$ .

The scattering matrix,  $\underline{\underline{F}}$ , governs the scattering of the locally defined Stokes parameters  $I_L$ ,  $I_x$ ,  $I_y$ ,  $U$ , and  $V$  and is constructed by considering the local scattering coordinate system shown in Figure 2.

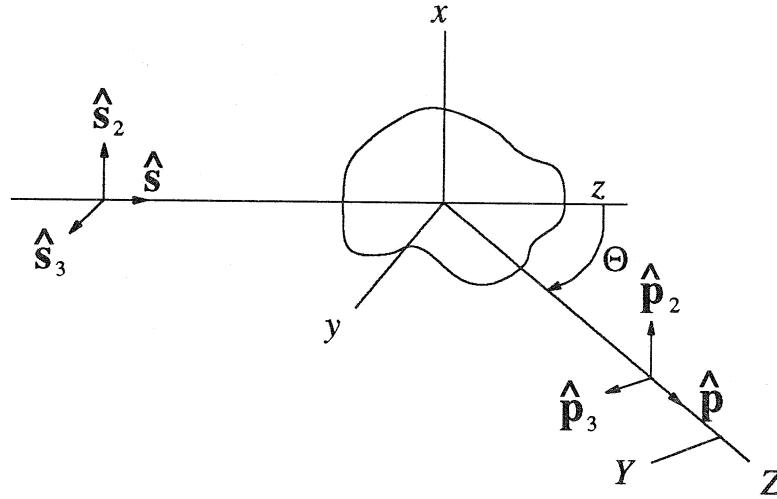


**Figure 2. Geometry for scattering in the local coordinate system.**

The incident ( $\hat{\mathbf{s}}$ ) and scattered ( $\hat{\mathbf{p}}$ ) directions are separated by an angle  $\Theta$  and define the plane of scattering. The  $\hat{\mathbf{s}}_2$  and  $\hat{\mathbf{p}}_2$  directions are parallel to each other and perpendicular to the plane of scattering and the  $\hat{\mathbf{s}}_3$  and  $\hat{\mathbf{p}}_3$  directions lie in the plane of scattering.



Using this coordinate system and the definition of a general inner product on  $\Xi$  given in Appendix A, the inner products required for  $F(\chi)$  are

$$\Xi \cdots \hat{\rho} \hat{\rho} \hat{s} \hat{s} = \frac{9}{525} + \frac{6}{525} \cos^2 \Theta + \frac{1}{525} \cos^4 \Theta, \quad (23)$$

$$\Xi \cdots \hat{\rho} \hat{\rho} \hat{s} \hat{s}_2 = \Xi \cdots \hat{\rho}_2 \hat{\rho} \hat{s} \hat{s} = \frac{5}{525} + \frac{5}{525} \cos^2 \Theta, \quad (24)$$

$$\Xi \cdots \hat{\rho} \hat{\rho} \hat{s} \hat{s}_3 = \Xi \cdots \hat{\rho}_3 \hat{\rho} \hat{s} \hat{s} = \frac{10}{525} + \frac{1}{525} \cos^2 \Theta - \frac{1}{525} \cos^4 \Theta, \quad (25)$$

$$\Xi \cdots \hat{\rho}_2 \hat{\rho} \hat{s} \hat{s}_2 = \frac{5}{525} + \frac{4}{525} \cos^2 \Theta, \quad (26)$$

$$\Xi \cdots \hat{\rho}_3 \hat{\rho} \hat{s} \hat{s}_3 = \frac{9}{525} - \frac{1}{525} \cos^2 \Theta + \frac{1}{525} \cos^4 \Theta, \quad (27)$$

$$\Xi \cdots \hat{\rho}_2 \hat{\rho} \hat{s} \hat{s}_3 = \Xi \cdots \hat{\rho}_3 \hat{\rho} \hat{s} \hat{s}_2 = \frac{5}{525}, \quad (28)$$

$$\Xi \cdots \hat{\rho}_2 \hat{\rho} \hat{s} \hat{s}_3 = \Xi \cdots \hat{\rho}_3 \hat{\rho} \hat{s} \hat{s}_3 = \frac{1}{525} \cos \Theta - \frac{2}{525} \cos^3 \Theta, \quad (29)$$

$$\Xi \cdots \hat{\rho}_2 \hat{\rho} \hat{s} \hat{s}_3 = \Xi \cdots \hat{\rho}_3 \hat{\rho} \hat{s} \hat{s}_2 = \frac{1}{210} \cos \Theta + \frac{1}{210} \cos^3 \Theta, \quad (30)$$

$$\Xi \cdots \hat{\rho}_2 \hat{\rho} \hat{s} \hat{s}_2 = \Xi \cdots \hat{\rho}_2 \hat{\rho} \hat{s} \hat{s}_3 = \Xi \cdots \hat{\rho}_3 \hat{\rho} \hat{s} \hat{s}_3 = \Xi \cdots \hat{\rho}_3 \hat{\rho} \hat{s} \hat{s}_2 = 0, \quad (31)$$

$$\Xi \cdots \hat{\rho}_3 \hat{\rho} \hat{s} \hat{s}_2 = \Xi \cdots \hat{\rho}_2 \hat{\rho} \hat{s} \hat{s}_3 = \Xi \cdots \hat{\rho}_3 \hat{\rho} \hat{s} \hat{s}_3 = \Xi \cdots \hat{\rho}_2 \hat{\rho} \hat{s} \hat{s}_3 = 0, \quad (32)$$

$$\Xi \cdots \hat{\rho} \hat{\rho} \hat{s} \hat{s}_2 = \Xi \cdots \hat{\rho}_2 \hat{\rho} \hat{s} \hat{s} = \Xi \cdots \hat{\rho} \hat{\rho} \hat{s} \hat{s}_3 = \Xi \cdots \hat{\rho}_3 \hat{\rho} \hat{s} \hat{s} = 0. \quad (33)$$

Note that with this choice of coordinates all necessary inner products are functions of  $\chi = \cos \Theta$  only as expected due to the assumed statistical isotropy of the medium.

Examining the quantities  $I_P$  and  $I_Q$  in comparison with the Stokes parameters  $U$  and  $V$  for discrete scatterers<sup>14</sup> leads to the conclusion

$$I_P + I_Q = U, \quad I_P - I_Q = V. \quad (34)$$

The local scattering matrix,  $\underline{\underline{F}}$ , for the five locally-defined Stokes parameters,  $I_L$ ,  $I_x$ ,  $I_y$ ,  $U$ , and  $V$  is then

$$\underline{\underline{F}} = \frac{2\pi^2\omega^4}{525} \begin{bmatrix} \frac{(9+6\chi^2+\chi^4)\eta^{LL}}{c_L^8} & \frac{5(1+\chi^2)\eta^{LT}}{c_L^5 c_T^3} & \frac{(10+\chi^2-\chi^4)\eta^{LT}}{c_L^5 c_T^3} & 0 & 0 \\ \frac{5(1+\chi^2)\eta^{LT}}{c_L^3 c_T^5} & \frac{(5+4\chi^2)\eta^{TT}}{c_T^8} & \frac{5}{c_T^8} \eta^{TT} & 0 & 0 \\ \frac{(10+\chi^2-\chi^4)\eta^{LT}}{c_L^3 c_T^5} & \frac{5}{c_T^8} \eta^{TT} & \frac{(9-\chi^2+\chi^4)\eta^{TT}}{c_T^8} & 0 & 0 \\ 0 & 0 & 0 & \frac{(7\chi+\chi^3)\eta^{TT}}{2c_T^8} & 0 \\ 0 & 0 & 0 & 0 & \frac{(-3\chi-9\chi^3)\eta^{TT}}{2c_T^8} \end{bmatrix} \quad (35)$$

where  $\chi = \cos \Theta$ . The Mueller matrix,  $\underline{\underline{P}}$ , is constructed according to Eq. (22). This matrix is given explicitly in Appendix B. It has the same properties and symmetries as  $\underline{\underline{P}}$  for the discrete scatterer case<sup>14</sup> and defines the scattering in terms of the globally-defined Stokes parameters,  $I_L$ ,  $I_{SV}$ ,  $I_{SH}$ ,  $U$ , and  $V$ .

Using the conservation of energy concepts given for the discrete scatterer URTE<sup>14</sup> we find the coherent intensity attenuations

$$\kappa_L = 2\alpha_L = \frac{1}{4\pi} \int P_{11} + P_{21} + P_{31} d^2\hat{\mathbf{p}}', \quad (36)$$

$$\kappa_T = 2\alpha_T = \frac{1}{8\pi} \int P_{12} + P_{13} + P_{22} + P_{23} + P_{32} + P_{33} d^2\hat{\mathbf{p}}'. \quad (37)$$

These attenuations, which are twice the respective displacement amplitude attenuations  $\alpha$  of the coherent field, are in agreement with Weaver<sup>13</sup> which agree with those given by Stanke and Kino<sup>21</sup> for an exponential two-point correlation function below the geometrical optics limit. Having the appropriate Mueller matrix for a cubic polycrystalline medium, we may now examine solutions to Eq. (21).

### III. SOLUTION OF THE URTE AND RESULTS

The Mueller matrix,  $\underline{P}$ , was derived for an exponential two-point correlation function of the form  $e^{-\beta r}$  where  $\beta^{-1}$  is some measure of the length scale of the scattering medium. In this case<sup>13</sup>

$$\begin{aligned}\eta^{LL}(\chi) &= \frac{v^2}{\beta^3 \pi^2} [1 + 2x_L^2(1 - \chi)]^{-2}, & \eta^{TT}(\chi) &= \frac{v^2}{\beta^3 \pi^2} [1 + 2x_T^2(1 - \chi)]^{-2}, \\ \eta^{LT}(\chi) &= \eta^{TL}(\chi) = \frac{v^2}{\beta^3 \pi^2} [1 + x_L^2 + x_T^2 - 2x_L x_T \chi]^{-2},\end{aligned}\tag{38}$$

where  $x_L = \omega/c_L \beta$  and  $x_T = \omega/c_T \beta$  are the dimensionless frequencies. The URTE given in Eq. (21) is nondimensionalized and solved using the discrete ordinates method as discussed for discrete scatterers.<sup>14</sup> Steady-state solutions are presented for a normally incident longitudinal wave. This type of incident field is axisymmetric so that the  $\phi$  dependence drops out leaving the intensity as a function of depth ( $z$ ) and  $\mu$ . Results are presented for polycrystalline iron with absorption effects neglected. The dimensionless depth,  $\tau = \kappa_T z$ , measures depth in units of inverse shear intensity attenuation. The dimensionless anisotropy factor for iron is  $v/\rho c_T^2 = -1.66$ , where  $\rho$  is the density.

The angular dependence of the intensities as a function of depth is shown in Figure 3 for  $x_T = 0.5$ . The horizontal line is included as a  $\mu = 0$  reference line denoting the separation between upward and downward propagating intensities. The solid line represents the longitudinal intensity,  $I_L$ , the small dashed line the shear vertical intensity,  $I_{SV}$ , and the large dashed line the shear horizontal intensity,  $I_{SH}$ . Note that the two shear intensities are nearly identical at all depths. The low frequency case has very smoothly varying intensities as a function of angle. At a depth of  $\tau = 20$  the intensities are nearly isotropic and are near the diffusive limit.

At a higher frequency,  $x_T = 3.5$ , as shown in Figure 4, a large forward scattering lobe is evident in the longitudinal intensity. This effect results in a depth greater than  $\tau = 40$  needed to achieve the isotropic diffusive limit.

The results shown in Figures 3 and 4 are indicative of other materials with similar Poisson's ratio in these dimensionless units. Thus, other results are not presented. The effect of the strength of the anisotropy is apparent when dimensional quantities are used. For example, the depth  $\tau = 20$  in which the low frequency solution reaches the diffusive limit is quite different in dimensional units for iron and aluminum which have very different degrees of anisotropy. For aluminum with  $\nu/\rho c_T^2 = -0.412$ , this diffusive depth is at  $76,000 \beta^{-1}$  while for iron it occurs at  $4600 \beta^{-1}$ . If we let  $\beta = 10/mm$ , then the excitation frequency,  $x_T = 0.5$  for both is about 2.5 MHz and the diffusive depths are 7.6 meters and 0.46 meters for aluminum and iron, respectively. For the higher frequency,  $x_T = 3.5$ , the excitation frequency for  $\beta = 10/mm$  is 17.4 and 18 MHz for aluminum and iron, respectively, and the diffusive depth at  $\tau = 40$  occurs at 15 cm for aluminum and 0.92 cm for iron. That large depths are required before the diffusion limit is reached has implications for difficulties in modeling diffuse energy evolution by means of a diffusion equation; in practice it seems that a radiative transfer equation will be required.



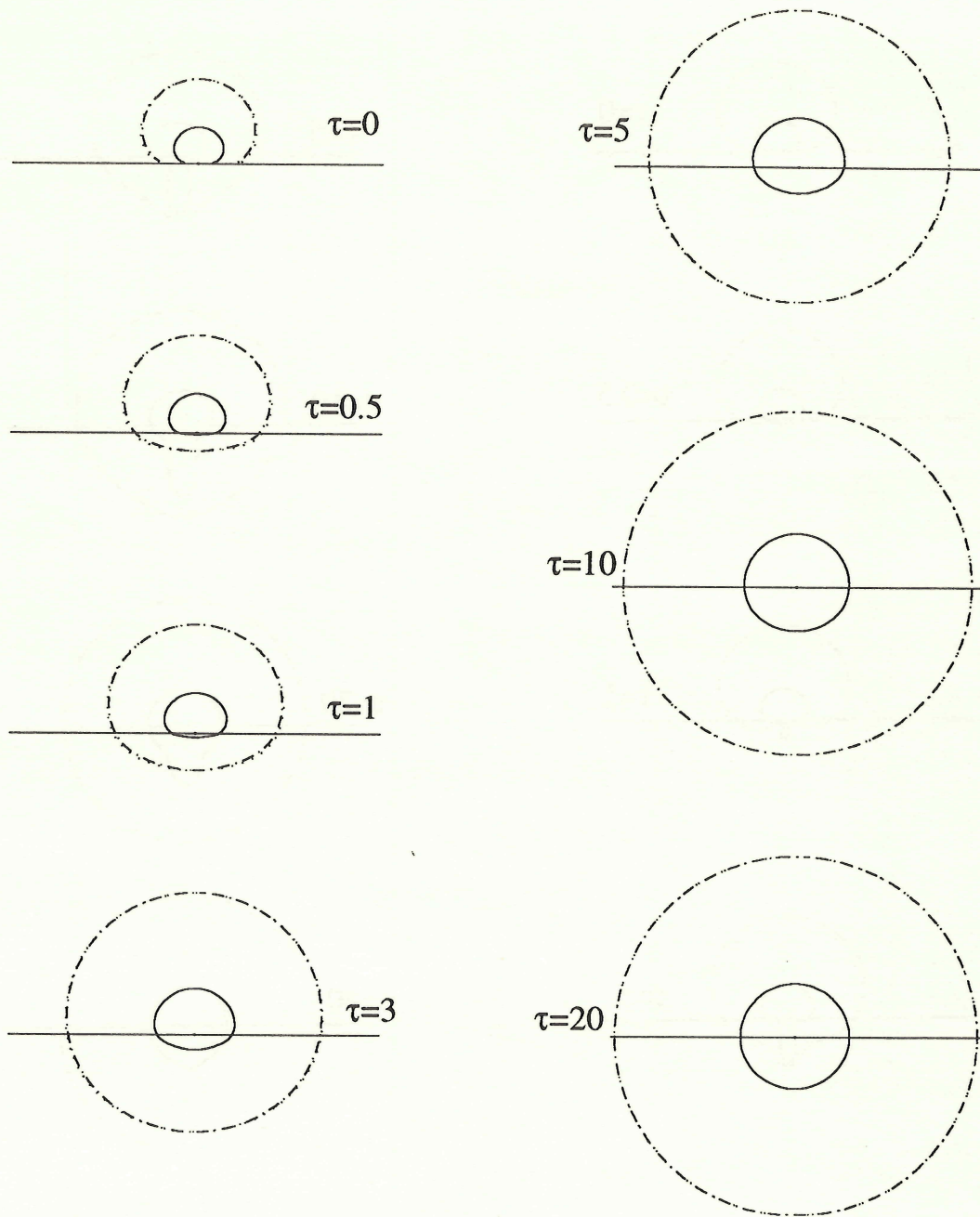


Figure 3. Angular dependence of intensity as a function of dimensionless depth for iron,  $x_T = 0.5$ , without absorption for the three modes  $I_L$  (solid line),  $I_{SV}$  (small dash), and  $I_{SH}$  (large dash). The two shear intensities are virtually indistinguishable at all depths.

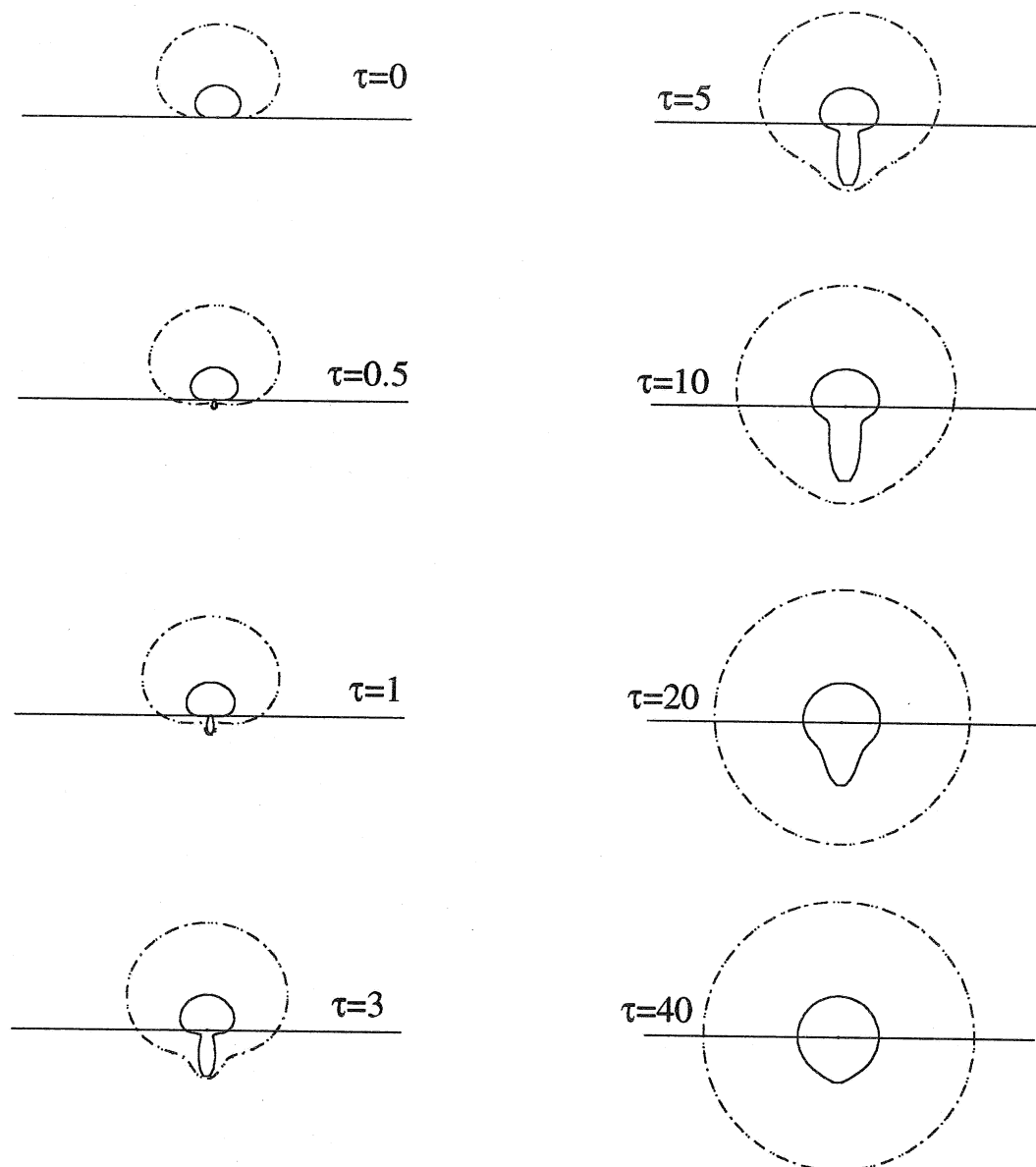


Figure 4. Angular dependence of intensity as a function of dimensionless depth for iron,  $x_T = 3.5$ , without absorption for the three modes  $I_L$  (solid line),  $I_{SV}$  (small dash), and  $I_{SH}$  (large dash). The two shear intensities are virtually indistinguishable for this frequency as well.

#### IV. CONCLUSIONS

Ultrasonic radiative transfer theory as developed for the discrete scatterer case has been extended to continuous polycrystalline media. The governing radiative transfer equation was derived by consideration of the ensemble averaged responses of the elastic wave equation. This may be contrasted with the energy balance arguments used for discrete scatterers. The ultrasonic radiative transfer equation is thus expected to be an accurate description of the multiply scattered ensemble averaged energy densities within the limits of the underlying assumptions, none of which are extensively prohibitive for most materials of interest. Results have been presented for steady-state insonification of a statistically homogeneous, statistically isotropic half space comprised of cubic crystallites. It has been found that the diffusion limit, often used to model multiply scattered ultrasound, is often achieved only at impractically great depths. The issues of time dependence and interface reflections, which are essential for comparison with experiments, will be discussed in a later communication.

#### ACKNOWLEDGEMENT

This work was sponsored by the National Science Foundation, Grant No. MSS-91-14360.

## REFERENCES

1. W. P. Mason and H. J. McSkimm, "Attenuation and scattering of high frequency sound waves in metals and glasses," *J. Acoust. Soc. Am.* **19**, 464-473 (1947).
2. A. B. Bhatia, "Scattering of high-frequency sound waves in polycrystalline materials," *J. Acoust. Soc. Am.* **19**, 16-23 (1959).
3. E. P. Papadakis, "Scattering in polycrystalline media," *Meth. Exp. Phys.* **19**, 237-298 (1981).
4. D. W. Fitting and L. Adler, *Ultrasonic Spectral Analysis for Nondestructive Evaluation* (Plenum Press, New York, 1981).
5. A. Vary, "Ultrasonic measurement of material properties," *Research Techniques in Nondestructive Testing V. IV*, edited by R. S. Sharpe (Academic Press, New York, 1980) pp. 159-204.
6. J. Saniie and N. M. Bilgutay, "Quantitative grain size evaluation using ultrasonic backscattered echoes," *J. Acoust. Soc. Am.* **80**, 1816-1824 (1986).
7. B. Fay, "Theoretical considerations of ultrasound backscatter," (in German) *Acustica* **28**, 354-357 (1973).
8. K. Goebbels, "Ultrasonics for microcrystalline structure examination," *Phil. Trans. R. Soc. Lond. A* **320**, 161-169 (1986).
9. F. J. Margetan, T. A. Gray, and R. B. Thompson, "A technique for quantitatively measuring microstructurally induced ultrasonic noise," *Review of Progress in Quantitative NDE, 10*, edited by D. O. Thompson and D. E. Chimenti (Plenum Press, New York, 1991) pp. 1721-1728.
10. J. H. Rose, "Ultrasonic backscatter from microstructure," *Review of Progress in Quantitative NDE, 11*, edited by D. O. Thompson and D. E. Chimenti (Plenum Press, New York, 1992) pp. 1677-1684.



11. M. D. Russell and S. P. Neal, "Grain noise power spectrum estimation for normal incidence ultrasonic interrogation of weak scattering polycrystalline materials using experimentally estimated longitudinal-wave backscatter coefficients," to be published in *Ultrasonics*.
12. C. B. Guo, P. Holler, and K. Goebbels, "Scattering of ultrasonic waves in anisotropic polycrystalline metals," *Acustica* **59**, 112-120 (1985).
13. R. L. Weaver, "Diffusivity of ultrasound in polycrystals," *J. Mech. Phys. Solids* **38**, 55-86 (1990).
14. J. A. Turner and R. L. Weaver, "Radiative transfer of ultrasound," TAM Report No. 725, September, 1993; J. A. Turner and R. L. Weaver, "Radiative transfer of ultrasound," submitted to *J. Acoust. Soc. Am.*
15. S. Chandrasekhar, *Radiative Transfer* (Dover, New York, 1960).
16. V. V. Sobolev, *A Treatise on Radiative Transfer* (D. Van Nostrand, New Jersey, 1963).
17. A. Ishimaru, *Wave Propagation and Scattering in Random Media* (Academic Press, New York, 1978), Vol. 1.
18. F. C. Karal and J. B. Keller, "Elastic, electromagnetic and other waves in random media," *J. Math. Phys.* **5**, 537-5447 (1964).
19. U. Frisch, "Wave propagation in random media," *Probablistic Methods in Applied Mathematics* edited by A. T. Bharucha-Reid (Academic Press, New York, 1968) Vol. 1, pp. 75-198.
20. J. J. McCoy, "Macroscopic response of continua with random microstructure," *Mechanics Today* edited by S. Nemat-Nasser (Pergamon Press, New York, 1981) Vol. 6.
21. F. E. Stanke and G. S. Kino, "A unified theory for elastic wave propagation in polycrystalline materials," *J. Acoust. Soc. Am.* **75**, 665-681 (1984).

## APPENDIX A

Certain inner products on the tensorial part of the covariance of the moduli fluctuations,  $\Xi$ , are required. For six arbitrary vectors  $\hat{s}$ ,  $\hat{p}$ ,  $\hat{u}$ ,  $\hat{v}$ ,  $\hat{q}$ , and  $\hat{r}$ ,

$$\begin{aligned} \Xi_{\dots\hat{p}\hat{s}\hat{q}}^{\dots\hat{u}\hat{p}\hat{s}\hat{q}} &= \Xi_{ijkl}^{\alpha\beta\gamma\delta} u_{\alpha} v_i p_{\beta} p_j s_{\gamma} s_k q_{\delta} r_l = \\ &b \{ (\hat{p} \cdot \hat{v}) (\hat{s} \cdot \hat{r}) + (\hat{s} \cdot \hat{v}) (\hat{p} \cdot \hat{r}) + (\hat{v} \cdot \hat{r}) (\hat{p} \cdot \hat{s}) \} \{ (\hat{p} \cdot \hat{u}) (\hat{s} \cdot \hat{q}) + (\hat{s} \cdot \hat{u}) (\hat{p} \cdot \hat{q}) + (\hat{u} \cdot \hat{q}) (\hat{p} \cdot \hat{s}) \} + \\ &h \{ (\hat{u} \cdot \hat{v}) (\hat{q} \cdot \hat{r}) + (\hat{u} \cdot \hat{v}) (\hat{s} \cdot \hat{q}) (\hat{s} \cdot \hat{r}) + (\hat{p} \cdot \hat{u}) (\hat{p} \cdot \hat{v}) (\hat{q} \cdot \hat{r}) + (\hat{p} \cdot \hat{u}) (\hat{p} \cdot \hat{v}) (\hat{s} \cdot \hat{q}) (\hat{s} \cdot \hat{r}) + \\ &(\hat{u} \cdot \hat{v}) (\hat{q} \cdot \hat{r}) (\hat{p} \cdot \hat{s})^2 + (\hat{u} \cdot \hat{v}) (\hat{p} \cdot \hat{s}) (\hat{s} \cdot \hat{q}) (\hat{p} \cdot \hat{r}) + (\hat{s} \cdot \hat{v}) (\hat{p} \cdot \hat{u}) (\hat{p} \cdot \hat{s}) (\hat{q} \cdot \hat{r}) + \\ &(\hat{s} \cdot \hat{v}) (\hat{p} \cdot \hat{u}) (\hat{s} \cdot \hat{q}) (\hat{p} \cdot \hat{r}) + (\hat{u} \cdot \hat{v}) (\hat{p} \cdot \hat{q}) (\hat{p} \cdot \hat{s}) (\hat{s} \cdot \hat{r}) + (\hat{u} \cdot \hat{v}) (\hat{p} \cdot \hat{q}) (\hat{p} \cdot \hat{r}) + \\ &(\hat{v} \cdot \hat{q}) (\hat{p} \cdot \hat{u}) (\hat{p} \cdot \hat{s}) (\hat{s} \cdot \hat{r}) + (\hat{v} \cdot \hat{q}) (\hat{p} \cdot \hat{u}) (\hat{p} \cdot \hat{r}) + (\hat{p} \cdot \hat{v}) (\hat{p} \cdot \hat{s}) (\hat{s} \cdot \hat{u}) (\hat{q} \cdot \hat{r}) + \\ &(\hat{p} \cdot \hat{v}) (\hat{p} \cdot \hat{s}) (\hat{s} \cdot \hat{q}) (\hat{u} \cdot \hat{r}) + (\hat{s} \cdot \hat{v}) (\hat{s} \cdot \hat{u}) (\hat{q} \cdot \hat{r}) + (\hat{s} \cdot \hat{v}) (\hat{s} \cdot \hat{q}) (\hat{u} \cdot \hat{r}) + \\ &(\hat{p} \cdot \hat{v}) (\hat{p} \cdot \hat{q}) (\hat{s} \cdot \hat{u}) (\hat{s} \cdot \hat{r}) + (\hat{p} \cdot \hat{v}) (\hat{p} \cdot \hat{q}) (\hat{u} \cdot \hat{r}) + (\hat{v} \cdot \hat{q}) (\hat{s} \cdot \hat{u}) (\hat{s} \cdot \hat{r}) + (\hat{v} \cdot \hat{q}) (\hat{u} \cdot \hat{r}) + \\ &(\hat{v} \cdot \hat{q}) (\hat{p} \cdot \hat{s}) (\hat{s} \cdot \hat{u}) (\hat{p} \cdot \hat{r}) + (\hat{v} \cdot \hat{q}) (\hat{u} \cdot \hat{r}) (\hat{p} \cdot \hat{s})^2 + \\ &(\hat{s} \cdot \hat{v}) (\hat{p} \cdot \hat{q}) (\hat{s} \cdot \hat{u}) (\hat{p} \cdot \hat{r}) + (\hat{s} \cdot \hat{v}) (\hat{p} \cdot \hat{q}) (\hat{p} \cdot \hat{s}) (\hat{u} \cdot \hat{r}) \} + \\ &d \{ (\hat{s} \cdot \hat{q}) [(\hat{u} \cdot \hat{v}) (\hat{s} \cdot \hat{r}) + (\hat{p} \cdot \hat{v}) (\hat{p} \cdot \hat{u}) (\hat{s} \cdot \hat{r}) + (\hat{s} \cdot \hat{u}) (\hat{p} \cdot \hat{r}) (\hat{p} \cdot \hat{v}) + (\hat{u} \cdot \hat{r}) (\hat{p} \cdot \hat{s}) (\hat{p} \cdot \hat{v}) + \\ &(\hat{p} \cdot \hat{u}) (\hat{p} \cdot \hat{r}) (\hat{s} \cdot \hat{v}) + (\hat{u} \cdot \hat{r}) (\hat{s} \cdot \hat{v}) + (\hat{p} \cdot \hat{u}) (\hat{p} \cdot \hat{s}) (\hat{v} \cdot \hat{r}) + (\hat{s} \cdot \hat{u}) (\hat{v} \cdot \hat{r}) + \\ &(\hat{u} \cdot \hat{v}) (\hat{p} \cdot \hat{r}) (\hat{p} \cdot \hat{s}) + (\hat{u} \cdot \hat{r}) (\hat{p} \cdot \hat{v}) (\hat{p} \cdot \hat{s}) + (\hat{u} \cdot \hat{v}) (\hat{p} \cdot \hat{s}) (\hat{p} \cdot \hat{r}) + (\hat{s} \cdot \hat{u}) (\hat{p} \cdot \hat{v}) (\hat{p} \cdot \hat{r})] + \\ &(\hat{p} \cdot \hat{u}) [(\hat{q} \cdot \hat{r}) (\hat{p} \cdot \hat{v}) + (\hat{s} \cdot \hat{v}) (\hat{p} \cdot \hat{q}) (\hat{s} \cdot \hat{r}) + (\hat{v} \cdot \hat{q}) (\hat{p} \cdot \hat{s}) (\hat{s} \cdot \hat{r}) + (\hat{s} \cdot \hat{r}) (\hat{s} \cdot \hat{q}) (\hat{p} \cdot \hat{v}) + \\ &(\hat{p} \cdot \hat{s}) (\hat{q} \cdot \hat{r}) (\hat{s} \cdot \hat{v}) + (\hat{s} \cdot \hat{r}) (\hat{p} \cdot \hat{q}) (\hat{s} \cdot \hat{v}) + (\hat{p} \cdot \hat{s}) (\hat{s} \cdot \hat{q}) (\hat{v} \cdot \hat{r}) + (\hat{p} \cdot \hat{q}) (\hat{v} \cdot \hat{r}) + \\ &(\hat{q} \cdot \hat{r}) (\hat{s} \cdot \hat{v}) (\hat{p} \cdot \hat{s}) + (\hat{s} \cdot \hat{r}) (\hat{v} \cdot \hat{q}) (\hat{p} \cdot \hat{s}) + (\hat{s} \cdot \hat{v}) (\hat{s} \cdot \hat{q}) (\hat{p} \cdot \hat{r}) + (\hat{v} \cdot \hat{q}) (\hat{p} \cdot \hat{r})] + \\ &(\hat{s} \cdot \hat{u}) [(\hat{v} \cdot \hat{q}) (\hat{s} \cdot \hat{r}) + (\hat{p} \cdot \hat{v}) (\hat{p} \cdot \hat{q}) (\hat{s} \cdot \hat{r}) + (\hat{p} \cdot \hat{s}) (\hat{q} \cdot \hat{r}) (\hat{p} \cdot \hat{v}) + (\hat{p} \cdot \hat{r}) (\hat{s} \cdot \hat{q}) (\hat{p} \cdot \hat{v}) + \\ &(\hat{q} \cdot \hat{r}) (\hat{s} \cdot \hat{v}) + (\hat{p} \cdot \hat{r}) (\hat{p} \cdot \hat{q}) (\hat{s} \cdot \hat{v}) + (\hat{s} \cdot \hat{q}) (\hat{v} \cdot \hat{r}) + (\hat{p} \cdot \hat{s}) (\hat{p} \cdot \hat{q}) (\hat{v} \cdot \hat{r}) + \\ &(\hat{p} \cdot \hat{v}) (\hat{q} \cdot \hat{r}) (\hat{p} \cdot \hat{s}) + (\hat{p} \cdot \hat{r}) (\hat{v} \cdot \hat{q}) (\hat{p} \cdot \hat{s}) + (\hat{p} \cdot \hat{v}) (\hat{s} \cdot \hat{q}) (\hat{p} \cdot \hat{r}) + (\hat{p} \cdot \hat{s}) (\hat{v} \cdot \hat{q}) (\hat{p} \cdot \hat{r})] + \end{aligned}$$

$$\begin{aligned}
& (\hat{u} \cdot \hat{q}) [(\hat{s} \cdot \hat{v})(\hat{s} \cdot \hat{r}) + (\hat{p} \cdot \hat{v})(\hat{p} \cdot \hat{s})(\hat{s} \cdot \hat{r}) + (\hat{p} \cdot \hat{s})(\hat{s} \cdot \hat{r})(\hat{p} \cdot \hat{v}) + (\hat{p} \cdot \hat{r})(\hat{p} \cdot \hat{v}) + \\
& \quad (\hat{s} \cdot \hat{r})(\hat{s} \cdot \hat{v}) + (\hat{p} \cdot \hat{r})(\hat{p} \cdot \hat{s})(\hat{s} \cdot \hat{v}) + (\hat{v} \cdot \hat{r}) + (\hat{v} \cdot \hat{r})(\hat{p} \cdot \hat{s})^2 + \\
& \quad (\hat{p} \cdot \hat{v})(\hat{s} \cdot \hat{r})(\hat{p} \cdot \hat{s}) + (\hat{p} \cdot \hat{r})(\hat{s} \cdot \hat{v})(\hat{p} \cdot \hat{s}) + (\hat{p} \cdot \hat{v})(\hat{p} \cdot \hat{r}) + (\hat{p} \cdot \hat{s})(\hat{s} \cdot \hat{v})(\hat{p} \cdot \hat{r})] + \\
& (\hat{p} \cdot \hat{q}) [(\hat{u} \cdot \hat{r})(\hat{p} \cdot \hat{v}) + (\hat{u} \cdot \hat{v})(\hat{p} \cdot \hat{s})(\hat{s} \cdot \hat{r}) + (\hat{s} \cdot \hat{v})(\hat{p} \cdot \hat{u})(\hat{s} \cdot \hat{r}) + (\hat{s} \cdot \hat{u})(\hat{s} \cdot \hat{r})(\hat{p} \cdot \hat{v}) + \\
& \quad (\hat{p} \cdot \hat{u})(\hat{s} \cdot \hat{r})(\hat{s} \cdot \hat{v}) + (\hat{u} \cdot \hat{r})(\hat{p} \cdot \hat{s})(\hat{s} \cdot \hat{v}) + (\hat{p} \cdot \hat{u})(\hat{v} \cdot \hat{r}) + (\hat{s} \cdot \hat{u})(\hat{p} \cdot \hat{s})(\hat{v} \cdot \hat{r}) + \\
& \quad (\hat{u} \cdot \hat{v})(\hat{s} \cdot \hat{r})(\hat{p} \cdot \hat{s}) + (\hat{u} \cdot \hat{r})(\hat{s} \cdot \hat{v})(\hat{p} \cdot \hat{s}) + (\hat{u} \cdot \hat{v})(\hat{p} \cdot \hat{r}) + (\hat{s} \cdot \hat{u})(\hat{s} \cdot \hat{v})(\hat{p} \cdot \hat{r})] + \\
& (\hat{p} \cdot \hat{s}) [(\hat{u} \cdot \hat{v})(\hat{p} \cdot \hat{q})(\hat{s} \cdot \hat{r}) + (\hat{v} \cdot \hat{q})(\hat{p} \cdot \hat{u})(\hat{s} \cdot \hat{r}) + (\hat{s} \cdot \hat{u})(\hat{q} \cdot \hat{r})(\hat{p} \cdot \hat{v}) + (\hat{u} \cdot \hat{r})(\hat{s} \cdot \hat{q})(\hat{p} \cdot \hat{v}) + \\
& \quad (\hat{p} \cdot \hat{u})(\hat{q} \cdot \hat{r})(\hat{s} \cdot \hat{v}) + (\hat{u} \cdot \hat{r})(\hat{p} \cdot \hat{q})(\hat{s} \cdot \hat{v}) + (\hat{p} \cdot \hat{u})(\hat{s} \cdot \hat{q})(\hat{v} \cdot \hat{r}) + (\hat{s} \cdot \hat{u})(\hat{p} \cdot \hat{q})(\hat{v} \cdot \hat{r}) + \\
& \quad (\hat{q} \cdot \hat{r})(\hat{u} \cdot \hat{v})(\hat{p} \cdot \hat{s}) + (\hat{u} \cdot \hat{r})(\hat{v} \cdot \hat{q})(\hat{p} \cdot \hat{s}) + (\hat{u} \cdot \hat{v})(\hat{s} \cdot \hat{q})(\hat{p} \cdot \hat{r}) + (\hat{s} \cdot \hat{u})(\hat{v} \cdot \hat{q})(\hat{p} \cdot \hat{r})] \} \quad (A1)
\end{aligned}$$

where  $b$ ,  $h$ , and  $d$  are given by Weaver for a cubic crystallite as  $2/1575$ ,  $1/180$ , and  $-1/630$ , respectively.

## APPENDIX B

The Mueller matrix for a cubic polycrystalline material is constructed from the local scattering matrix,  $\underline{\underline{F}}$ , using Eq. (22). The result is

$$\underline{\underline{P}}(\mu, \phi; \mu', \phi') = \begin{bmatrix} P_{11} & P_{12} & P_{13} & P_{14} & 0 \\ P_{21} & P_{22} & P_{23} & P_{24} & 0 \\ P_{31} & P_{32} & P_{33} & P_{34} & 0 \\ P_{41} & P_{42} & P_{43} & P_{44} & 0 \\ 0 & 0 & 0 & 0 & P_{55} \end{bmatrix}, \quad (\text{B1})$$

where

$$P_{11} = \frac{2\pi^2\omega^4}{525c_L^8} \eta^{LL}(\chi) [9 + 6\chi^2 + \chi^4], \quad (\text{B2})$$

$$P_{12} = \frac{2\pi^2\omega^4}{525c_L^5c_T^3} \eta^{TL}(\chi) [5(1 + \chi^2) \sin^2 \beta + (10 + \chi^2 - \chi^4) \cos^2 \beta], \quad (\text{B3})$$

$$P_{13} = \frac{2\pi^2\omega^4}{525c_L^5c_T^3} \eta^{TL}(\chi) [5(1 + \chi^2) \cos^2 \beta + (10 + \chi^2 - \chi^4) \sin^2 \beta], \quad (\text{B4})$$

$$P_{14} = \frac{2\pi^2\omega^4}{525c_L^5c_T^3} \eta^{TL}(\chi) [5 - 4\chi^2 - \chi^4] \sin 2\beta, \quad (\text{B5})$$

$$P_{21} = \frac{2\pi^2\omega^4}{525c_L^3c_T^5} \eta^{LT}(\chi) [5(1 + \chi^2) \sin^2 \gamma + (10 + \chi^2 - \chi^4) \cos^2 \gamma], \quad (\text{B6})$$

$$P_{22} = \frac{2\pi^2\omega^4}{525c_T^8} \eta^{TT}(\chi) \left\{ [5 + 4\chi^2 \sin^2 \gamma] \sin^2 \beta + [5 \sin^2 \gamma + (9 - \chi^2 + \chi^4) \cos^2 \gamma] \cos^2 \beta - \frac{1}{4} [7\chi + \chi^3] \sin 2\gamma \sin 2\beta \right\}, \quad (\text{B7})$$



$$P_{23} = \frac{2\pi^2\omega^4}{525c_T^8}\eta^{TT}(\chi)\left\{ [5 + 4\chi^2\sin^2\gamma]\cos^2\beta + [5\sin^2\gamma + (9 - \chi^2 + \chi^4)\cos^2\gamma]\sin^2\beta + \right. \\ \left. \frac{1}{4}[7\chi + \chi^3]\sin 2\gamma\sin 2\beta \right\}, \quad (\text{B8})$$

$$P_{24} = \frac{2\pi^2\omega^4}{525c_T^8}\eta^{TT}(\chi)\left\{ [-4\chi^2\sin^2\gamma + (4 - \chi^2 + \chi^4)\cos^2\gamma]\frac{1}{2}\sin 2\beta + \frac{1}{4}[7\chi + \chi^3]\sin 2\gamma\cos 2\beta \right\}, \quad (\text{B9})$$

$$P_{31} = \frac{2\pi^2\omega^4}{525c_L^3c_T^5}\eta^{LT}(\chi)[5(1 + \chi^2)\cos^2\gamma + (10 + \chi^2 - \chi^4)\sin^2\gamma], \quad (\text{B10})$$

$$P_{32} = \frac{2\pi^2\omega^4}{525c_T^8}\eta^{TT}(\chi)\left\{ [5 + 4\chi^2\cos^2\gamma]\sin^2\beta + [5\cos^2\gamma + (9 - \chi^2 + \chi^4)\sin^2\gamma]\cos^2\beta + \right. \\ \left. \frac{1}{4}[7\chi + \chi^3]\sin 2\gamma\sin 2\beta \right\}, \quad (\text{B11})$$

$$P_{33} = \frac{2\pi^2\omega^4}{525c_T^8}\eta^{TT}(\chi)\left\{ [5 + 4\chi^2\cos^2\gamma]\cos^2\beta + [5\cos^2\gamma + (9 - \chi^2 + \chi^4)\sin^2\gamma]\sin^2\beta - \right. \\ \left. \frac{1}{4}[7\chi + \chi^3]\sin 2\gamma\sin 2\beta \right\}, \quad (\text{B12})$$

$$P_{34} = \frac{2\pi^2\omega^4}{525c_T^8}\eta^{TT}(\chi)\left\{ [-4\chi^2\cos^2\gamma + (4 - \chi^2 + \chi^4)\sin^2\gamma]\frac{1}{2}\sin 2\beta - \frac{1}{4}[7\chi + \chi^3]\sin 2\gamma\cos 2\beta \right\}, \quad (\text{B13})$$

$$P_{41} = \frac{2\pi^2\omega^4}{525c_L^3c_T^5}\eta^{LT}(\chi)[-5 + 4\chi^2 + \chi^4]\sin 2\gamma, \quad (\text{B14})$$

$$P_{42} = \frac{2\pi^2\omega^4}{525c_T^8}\eta^{TT}(\chi)\left\{ [4\chi^2\sin^2\beta + (-4 + \chi^2 - \chi^4)\cos^2\beta]\sin 2\gamma - \frac{1}{2}[7\chi + \chi^3]\cos 2\gamma\sin 2\beta \right\}, \quad (\text{B15})$$

$$P_{43} = \frac{2\pi^2\omega^4}{525c_T^8}\eta^{TT}(\chi)\left\{ [4\chi^2\cos^2\beta + (-4 + \chi^2 - \chi^4)\sin^2\beta]\sin 2\gamma + \frac{1}{2}[7\chi + \chi^3]\cos 2\gamma\sin 2\beta \right\}, \quad (\text{B16})$$

$$P_{44} = \frac{2\pi^2\omega^4}{1050c_T^8} \eta^{TT}(\chi) [(7\chi + \chi^3) \cos 2\gamma \cos^2 \beta - (4 + 3\chi^2 + \chi^4) \sin 2\gamma \sin 2\beta], \quad (\text{B17})$$

$$P_{55} = \frac{2\pi^2\omega^4}{1050c_T^8} \eta^{TT}(\chi) [-3\chi - 9\chi^3], \quad (\text{B18})$$

with

$$\begin{aligned} \cos \beta &= \frac{1}{\sqrt{1-\chi^2}} [\mu' \sqrt{1-\mu'^2} - \mu' \sqrt{1-\mu'^2} \cos(\phi' - \phi)], \\ \sin \beta &= \sqrt{\frac{1-\mu'^2}{1-\chi^2}} \sin(\phi' - \phi), \\ \cos \gamma &= \frac{1}{\sqrt{1-\chi^2}} [\mu' \sqrt{1-\mu'^2} - \mu \sqrt{1-\mu'^2} \cos(\phi' - \phi)], \\ \sin \gamma &= \sqrt{\frac{1-\mu'^2}{1-\chi^2}} \sin(\phi' - \phi), \end{aligned} \quad (\text{B19})$$

$$\text{and } \chi = \cos \Theta = \mu\mu' + \sqrt{1-\mu^2} \sqrt{1-\mu'^2} \cos(\phi' - \phi).$$

## List of Recent TAM Reports

<i>No.</i>	<i>Authors</i>	<i>Title</i>	<i>Date</i>
711	Weaver, R. L.	Anderson localization in the time domain: Numerical studies of waves in two-dimensional disordered media	Apr. 1993
712	Cherukuri, H. P., and T. G. Shawki	An energy-based localization theory: Part I—Basic framework	Apr. 1993
713	Manring, N. D., and R. E. Johnson	Modeling a variable-displacement pump	June 1993
714	Birnbaum, H. K., and P. Sofronis	Hydrogen-enhanced localized plasticity—A mechanism for hydrogen-related fracture	July 1993
715	Balachandar, S., and M. R. Malik	Inviscid instability of streamwise corner flow	July 1993
716	Sofronis, P.	Linearized hydrogen elasticity	July 1993
717	Nitzsche, V. R., and K. J. Hsia	Modelling of dislocation mobility controlled brittle-to-ductile transition	July 1993
718	Hsia, K. J., and A. S. Argon	Experimental study of the mechanisms of brittle-to-ductile transition of cleavage fracture in silicon single crystals	July 1993
719	Cherukuri, H. P., and T. G. Shawki	An energy-based localization theory: Part II—Effects of the diffusion, inertia and dissipation numbers	Aug. 1993
720	Aref, H., and S. W. Jones	Chaotic motion of a solid through ideal fluid	Aug. 1993
721	Stewart, D. S.	Lectures on detonation physics: Introduction to the theory of detonation shock dynamics	Aug. 1993
722	Lawrence, C. J., and R. Mei	Long-time behavior of the drag on a body in impulsive motion	Sept. 1993
723	Mei, R., J. F. Klausner, and C. J. Lawrence	A note on the history force on a spherical bubble at finite Reynolds number	Sept. 1993
724	Qi, Q., R. E. Johnson, and J. G. Harris	A re-examination of the boundary layer attenuation and acoustic streaming accompanying plane wave propagation in a circular tube	Sept. 1993
725	Turner, J. A., and R. L. Weaver	Radiative transfer of ultrasound	Sept. 1993
726	Yogeswaren, E. K., and J. G. Harris	A model of a confocal ultrasonic inspection system for interfaces	Sept. 1993
727	Yao, J., and D. S. Stewart	On the normal detonation shock velocity-curvature relationship for materials with large activation energy	Sept. 1993
728	Qi, Q.	Attenuated leaky Rayleigh waves	Oct. 1993
729	Sofronis, P., and H. K. Birnbaum	Mechanics of hydrogen-dislocation-impurity interactions: Part I—Increasing shear modulus	Oct. 1993
730	Hsia, K. J., Z. Suo, and W. Yang	Cleavage due to dislocation confinement in layered materials	Oct. 1993
731	Acharya, A., and T. G. Shawki	A second-deformation-gradient theory of plasticity	Oct. 1993
732	Michaleris, P., D. A. Tortorelli, and C. A. Vidal	Tangent operators and design sensitivity formulations for transient nonlinear coupled problems with applications to elasto-plasticity	Nov. 1993
733	Michaleris, P., D. A. Tortorelli, and C. A. Vidal	Analysis and optimization of weakly coupled thermo-elasto-plastic systems with applications to weldment design	Nov. 1993
734	Ford, D. K., and D. S. Stewart	Probabilistic modeling of propellant beds exposed to strong stimulus	Nov. 1993
735	Mei, R., R. J. Adrian, and T. J. Hanratty	Particle dispersion in isotropic turbulence under the influence of non-Stokesian drag and gravitational settling	Nov. 1993
736	Dey, N., D. F. Socie, and K. J. Hsia	Static and cyclic fatigue failure at high temperature in ceramics containing grain boundary viscous phase: Part I—Experiments	Nov. 1993
737	Dey, N., D. F. Socie, and K. J. Hsia	Static and cyclic fatigue failure at high temperature in ceramics containing grain boundary viscous phase: Part II—Modelling	Nov. 1993
738	Turner, J. A., and R. L. Weaver	Radiative transfer and multiple scattering of diffuse ultrasound in polycrystalline media	Nov. 1993

